

Engineering Notes

Experimental Verification of Periodic Libration of Tethered Satellite System in Elliptic Orbit

Hirohisa Kojima* and Yoshiyasu Furukawa†
Tokyo Metropolitan University,
Hino, Tokyo 191-0065, Japan

and
Pavel M. Trivailo‡

Royal Melbourne Institute of Technology,
Melbourne, Victoria 3083, Australia

DOI: 10.2514/1.52399

Nomenclature

| | | |
|-----------------|---|--|
| a | = | semimajor axis, m |
| e | = | eccentricity |
| g | = | gravitational acceleration on the ground, 9.8 m/s ² |
| I_1, I_2, I_3 | = | centroidal principal moment of inertia of the tethered satellite system, kg · m ² |
| k_2 | = | inertia ratio of the tethered satellite system, $k_2 := (I_1 - I_3)/I_2$ |
| l | = | tether length, m |
| m | = | subsattellite mass, kg |
| n | = | mean orbital rate, $\sqrt{\mu/a^3}$ rad/s |
| R | = | orbital radius, m |
| r_a | = | apoapsis distance, m |
| r_p | = | periapsis distance, m |
| η | = | true anomaly, rad |
| θ | = | tether pitch angle, rad |
| μ | = | Earth gravitational constant, 3.98613×10^5 km ³ /s ² |
| ϕ | = | inclination angle of the turntable, rad |
| \int | = | $d(\cdot)/d\eta$ |

I. Introduction

TETHERED satellite systems are often considered as revolutionary new technologies capable of solving complex tasks for challenging future space missions such as construction of large space structures, momentum exchange [1], debris elimination [2], artificial gravity generation by rotational motion, and so on [3]. To make the application of tethered satellite systems feasible, their dynamics and control must be comprehensively understood and properly addressed.

Presented as Paper 2009-5815 at the Modeling and Simulation Technology, Chicago, IL, 9–13 August 2009; received 15 September 2010; revision received 9 November 2010; accepted for publication 11 November 2010. Copyright © 2010 by Hirohisa Kojima, Yoshiyasu Furukawa, and Pavel M. Trivailo. Published by the American Institute of Aeronautics and Astronautics, Inc., with permission. Copies of this paper may be made for personal or internal use, on condition that the copier pay the \$10.00 per-copy fee to the Copyright Clearance Center, Inc., 222 Rosewood Drive, Danvers, MA 01923; include the code 0731-5090/11 and \$10.00 in correspondence with the CCC.

*Professor, Department of Aerospace Engineering; hkojima@sd.tmu.ac.jp. Senior Member AIAA.

†Graduate Student, Department of Aerospace Engineering; furukawa-yoshiyasu@sd.tmu.ac.jp.

‡Professor, School of Aerospace, Mechanical, and Manufacturing Engineering; pavel.trivailo@rmit.edu.au.

In the past, ground-based experimental setups have been constructed to study dynamics and control of tethered satellite systems experimentally. In particular, a case of a tethered subsatellite retrieval to and deployment from the mother satellite in circular orbits has been considered in detail [4,5].

Librational motion of tethered satellite systems in elliptic orbits is much more complex than in the case of circular orbits: it is very much dependent upon the magnitude of the orbit's eccentricity, and may vary from periodic to chaotic motion. It is well known that librational motion of tethered satellite systems in elliptic orbits starts tumbling around eccentricity of 0.355 [6]. This interesting result has inspired researchers to investigate the chaotic librational motions of tethered satellite systems in elliptic orbits, mostly numerically.

Karasopoulos and Richardson [7] have obtained in-plane periodic solutions for non electrodynamic rigid tethers in elliptic orbits, and have analyzed their characteristics using Poincaré map and bifurcation theory. Peláez et al. have obtained periodic motion for electrodynamic tether systems in inclined elliptic orbits [8], and analyzed their stability [9]. Applications of delayed feedback control [10] to chaotic librational motion of tethered systems have been studied in [11–15].

Many interesting results have been already presented and summarized in the previous publications. However, to the best knowledge of the authors, chaotic librational motions of tether satellite systems in elliptic orbits have not yet been studied experimentally by developing an experimental setup that can emulate pitching motion of a tethered satellite system in elliptic orbits on the ground. Because periodic motions are concerned for new types of space missions involving tethered satellite systems, they should be studied not only numerically but also experimentally to ensure that they are achievable.

In this Note, as the first step toward validation of the previously introduced control schemes, the ground-based experimental setup is proposed and designed to emulate pitch motions of a tethered satellite system in elliptic orbits. The experimental setup consists of four movable parts driven by stepper motors, one of which is an inclined turntable to emulate a gravity gradient. A mathematical model based on the experimental setup is derived, and the inclined angle of the turntable is determined in accordance with the orbital motion to emulate the gravity gradient torque. The results of numerical simulations and experiments demonstrate that the experimental setup can emulate chaotic pitching motions of a tethered satellite system in elliptic orbits.

II. Chaotic Motion of Tethered System in Elliptic Orbit

A. Equation of Pitch Motion

To investigate the effect of gravity on the motion of the tethered satellite system, the elasticity of the tether and the aerodynamic drag force affecting the system are assumed to be negligible, and only the station-keeping phase and in-plane motions are considered in this Note.

The motion of the tethered satellite system is classified into two types: librational motion and rotational motion. The tethered satellite swings like a pendulum in the case of librational motion and rotates around the center of mass in the case of rotational motion. The schematic model of the tethered satellite system treated in this Note is illustrated in Fig. 1. This system consists of a mother satellite, a subsatellite, and a tether connecting these satellites. The mother satellite and the subsatellite are assumed to be particles with masses, and the tether is assumed to be a rigid body without mass or inertia. In other words, the tethered satellite in this Note is assumed to be a dumbbell model. Tether length is assumed to be much shorter than

the orbital radius and denoted by l . It is assumed that the mass of the mother satellite is much greater than that of the subsatellite, and that the center of mass of the system follows a Keplerian elliptic orbit whose orbital radius is denoted by R . The parameters η , and θ are the true anomaly of the center of mass of the system, and the angle of the tether relative to the direction to the center of the Earth, respectively.

Because we assume a dumbbell model for the tethered satellite system, that is $I_1 = I_2$, $I_3 = 0$, the system inertia ratio, $k_2 := (I_1 - I_3)/I_2 = 1$. Under these assumptions, simplifying the gravity gradient, replacing the independent variable time t with the true anomaly η , and applying the Lagrange method yields the equation of pitch motion, as follows [16]:

$$(1 + e \cos \eta)\theta'' - (2e \sin \eta)\theta' + 3 \sin \theta \cos \theta = 2e \sin \eta \quad (1)$$

B. Bifurcation Diagram

Bifurcation occurs when a fixed point on the Poincaré map is not a saddle fixed point, which indicates structural instability. The dynamics around the saddle fixed point is changed dramatically by perturbation and brings about a qualitative change in the motion. For example, a fixed point may disappear and new fixed points may appear, or the periodic motion may change to chaotic motion due to the perturbation. A bifurcation diagram is a chaos analysis tool, and can be used to find periodic motions. When it is used for tethered satellite systems in elliptic orbits by changing the eccentricity, it indicates the type of motion that occurs for a range of eccentricities and for specific initial conditions. The bifurcation diagram is constructed by periodically sampling points in the same way as a Poincaré map and is plotted with respect to eccentricity. Figure 2 shows a bifurcation diagram for the attitude of the tethered satellite system during 1000 orbits with the initial conditions of $(\theta, \dot{\theta}) = (0, 0)$. This figure shows the relationship between θ and e . The periodic motion diverges as eccentricity increases and becomes chaotic in the vicinity of approximately $e = 0.3138$. A similar value was firstly reported in [6]. Periodic motions with periods of 3, 8, 5, 12, and 7 orbits appear at $e = 0.24966, 0.28945, 0.30146, 0.31023$, and 0.31309 , respectively. Table 1 lists the periods of these motions as well as one another periodic motion that was found from the bifurcation diagram. These are almost the same as those reported in [7].

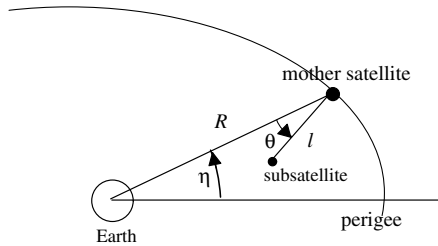


Fig. 1 Tethered satellite system in elliptic orbit.

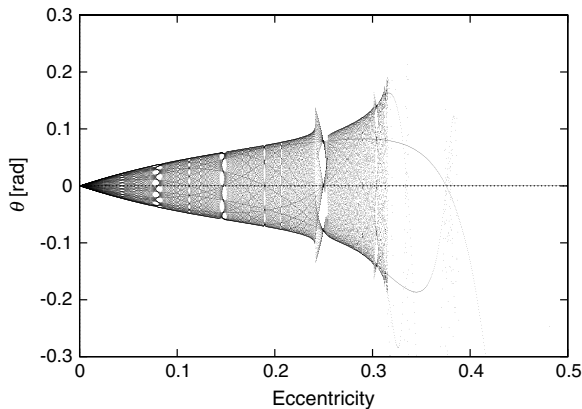


Fig. 2 Bifurcation diagram, tether angle vs eccentricity.

Table 1 List of periodic motions and corresponding eccentricities

| Period (orbits) | Eccentricity |
|-----------------|--------------|
| 11 | 0.07997 |
| 3 | 0.24966 |
| 8 | 0.28945 |
| 5 | 0.30416 |
| 12 | 0.31023 |
| 7 | 0.31309 |

III. Experimental Setup

In this section, we will describe the experimental setup developed for studying the tether's in-plane librational motion in elliptic orbits[17].

A. Conceptual Design

Higuchi and Natori [4] in 1999 and Koga [5] in 1998 developed systems to study the dynamics and control of tethered systems in circular orbits. Their systems were, however, mainly used to study the deployment and retrieval phase of tether motion, and were not able to emulate elliptic orbits.

To overcome this problem, an advanced system has been designed. Figure 3 shows a conceptual design of the ground-based experimental setup to study tether chaotic motion [17]. Because it is impossible to emulate both the in-plane and out-plane motions on the ground, the experimental setup is intended to emulate the in-plane motion only. The experimental setup is characterized with the following features:

- 1) It contains a rotating plate driven by a motor connected to the main shaft to emulate orbital motion.
- 2) Its table is inclined to emulate the Earth's gravity.
- 3) It contains a reel mechanism to control tether length.
- 4) Its parallel slider is equipped with a motor to emulate the change of the orbital radius of the mother satellite.

B. Sizing and Modeling of Experimental Setup

The dimensions of the experimental apparatus are specifically selected to emulate the elliptic motion of the mother satellite model, and the gravity gradient affecting the subsatellite. To determine the appropriate dimensions, not only the dependency among orbital parameters, but also some constraints (such as the experiment room size) should be taken into consideration. In this work, a top-down procedure was used to determine the optimum dimensions of the components in the apparatus.

Firstly, taking the available area in the laboratory into account, it was decided that the apparatus should fit within a $2.0 \times 2.0 \times 2.0$ m cube. Secondly, the size of the rectangular turntable was

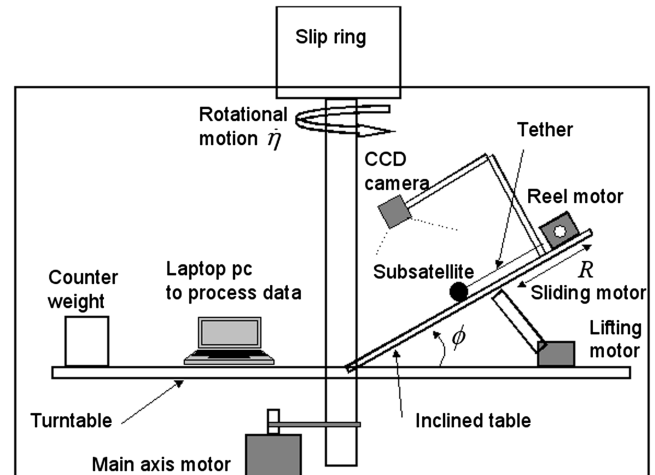


Fig. 3 Schematic representation of the experimental setup.

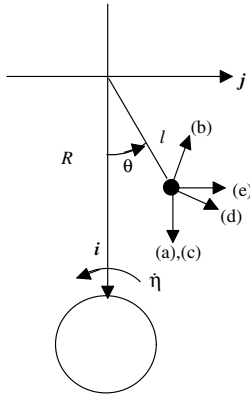


Fig. 4 Schematic representation of forces affecting the tethered subsatellite in orbit.

determined to be 0.80 m long \times 0.30 m wide, allowing for a margin of 0.15 m from the walls, and 0.05 m from the center shaft. On the basis of the results shown in Fig. 2, or in [7], the ability to simulate eccentricity values up to approximately 0.35 should be sufficient to promote chaotic librational motion in the experimental setup. Using the periapsis distance r_p and the apoapsis distance r_a , eccentricity is given by

$$e = (r_a - r_p) / (r_a + r_p) \quad (2)$$

To allow some margin at the ends of the turntable, the apogee radius r_a was assumed to be approximately 90% of the turntable length, and the perigee radius corresponding to an eccentricity of 0.35 was then obtained as

$$r_p = \frac{(1 - e)r_a}{1 + e} = \frac{(1 - 0.35) \times 0.75}{1 + 0.35} = 0.361 \text{ [m]}$$

As a result, the movable range of the slider was selected to be 0.35–0.75 m to emulate the elliptic orbits in which the mother satellite moves.

As far as possible, it is necessary to assign practical values to the nondimensional force affecting the subsatellite in order to emulate the in-plane tethered subsatellite motion in elliptic orbits. For this purpose, we need to consider the orbital radius, the first and second time derivatives of the orbital radius and the true anomaly. The forces affecting the subsatellite are gravity, centrifugal force, Coriolis force, inertia force induced by the true anomaly acceleration, and orbital radial acceleration. Setting the coordinate (\mathbf{i}, \mathbf{j}) on the mother satellite as shown in Fig. 4, these forces on a subsatellite with a mass of m can be written, respectively, as 1) gravity equals $mg \sin \phi \mathbf{i}$; 2) centrifugal force equals $-m(R - l \cos \theta) \dot{\eta}^2 \cos^2 \phi \mathbf{i} + ml \sin \theta \dot{\eta}^2 \mathbf{j}$; 3) inertial force due to radial acceleration equals $m \ddot{R} \mathbf{i}$; 4) inertial force due to true anomaly acceleration equals $ml \sin \theta \cos \phi \ddot{\eta} \mathbf{i} + m(R - l \cos \theta) \cos \phi \ddot{\eta} \mathbf{j}$; and 5) Coriolis force equals $2m \dot{R} \dot{\eta} \cos \phi \mathbf{j}$.

Taking into account the torques affecting the tethered satellite system around the origin induced by the preceding forces, the equation of pitch motion of the tethered satellite system on the experimental setup is obtained as

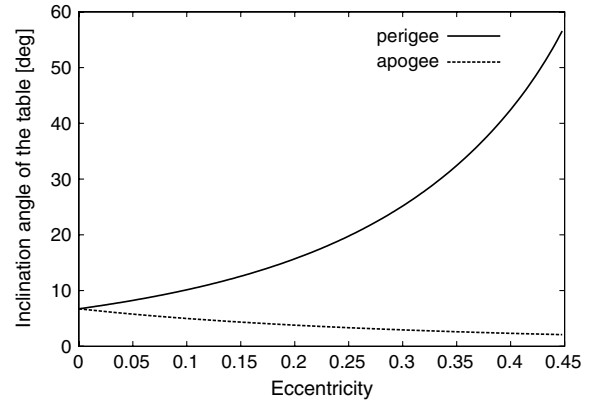


Fig. 5 Inclination angle of the turntable vs eccentricity.

$$\begin{aligned} ml^2 \ddot{\theta} = & ml[-\ddot{R} + (R - l \cos \theta) \dot{\eta}^2 \cos^2 \phi - g \sin \phi] \sin \theta \\ & + ml[2\dot{R} \dot{\eta} \cos \phi + R \ddot{\eta} \cos \phi] \cos \theta - ml^2 \dot{\eta} \cos \phi \\ & + ml^2 \dot{\eta}^2 \sin \theta \cos \theta \end{aligned} \quad (3)$$

The inclination angle of the turntable in Eq. (3), ϕ , is a free parameter, and should be controlled appropriately to emulate the gravity gradient affecting the subsatellite. To achieve this objective, assuming that the gravity gradient torque on the orbit, T_{g1} , which is given by

$$T_{g1} = -3mn^2 l^2 \sin \theta \cos \theta \quad (4)$$

and the gravity gradient torque in the experimental setup, T_{g2} , which is given by

$$T_{g2} = ml(R \dot{\eta}^2 \cos^2 \phi - g \sin \phi) \sin \theta + ml^2 \dot{\eta}^2 \sin^2 \phi \sin \theta \cos \theta \quad (5)$$

are the same, that the tether angle is small, and that the mean orbital rate n is approximately the same as the orbital rate $\dot{\eta}$, the inclination angle of the table is then calculated as

$$\phi(\eta) = \sin^{-1} \{ \{-g + \sqrt{g^2 + 4\dot{\eta}^4 (R - l)(R + 3l)}\} / 2(R - l) \dot{\eta}^2 \} \} \quad (6)$$

Figure 5 shows the inclination angle at the perigee and apogee vs eccentricity, under example conditions that the tether length is 0.15 m, the mean orbital rate n is 1.2 rad/s, and the perigee radius is 0.35 m in the experimental setup. Although the tether is assumed to be rigid in this study, a cotton thread is employed as the tether in the experiments. To emulate the gravity gradient successfully for a range of eccentricity from 0 to 0.35, the inclination must be changed from 3 to 35 deg. The preceding example conditions are selected by taking into account the clearance between the subsatellite and the center shaft, and the safety limits on the rotational speed. Note that the mean orbital rate and tether length in the apparatus can be changed in accordance with the research objective. Consequently, the principal dimensions and specifications of the experimental apparatus are summarized in Table 2.

Table 2 Configuration of the experimental setup

| Parameter | Value |
|--|----------------------------------|
| Width, depth, height of the setup | 2.0 \times 2.0 \times 2.0 m |
| Width and length of the turntable | 0.3 \times 0.8 m |
| Movable range of the slider | 0.35–0.75 m |
| Inclination angle range | 3–40 deg |
| Mean orbital rate | 1.2 rad/s |
| Tether length and material | 0.15 m, cotton thread |
| Charge-coupled-device camera | Logicool QCAM-200V (200M pixels) |
| Subsatellite weight (including dry ice) | 0.07 \pm 0.01 kg |
| Damping ratio due to friction (case of 15 deg inclination angle) | 1.97 $\times 10^{-2}$ |

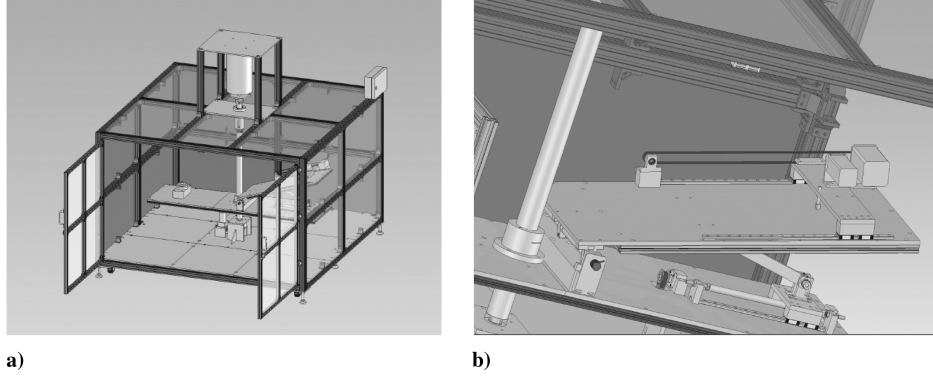


Fig. 6 Experimental setup: a) apparatus and b) inclined turntable.

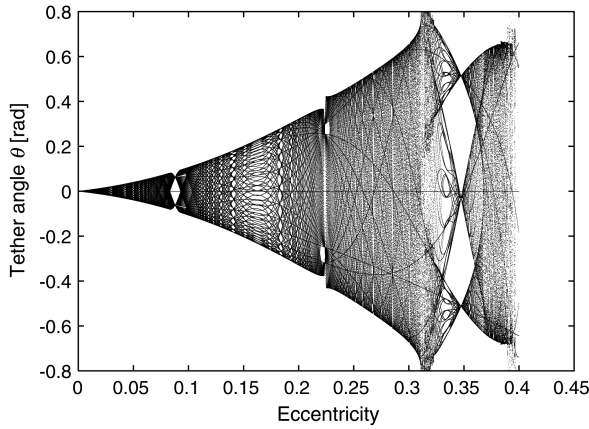


Fig. 7 Bifurcation diagram resulting from the numerical simulations based on the experimental setup.

Using the preceding determined parameters, the experimental setup was constructed. Figure 6a shows the experimental apparatus, and Fig. 6b shows a close-up of the inclined turntable. Each movable part is driven by a stepper motor manufactured by Oriental Motor Co., Ltd. The inclination angle of the turntable is changed using a jackscrew, as shown in Fig. 6b. The electric signals and current are provided to the motors through a slip ring device installed on the top of the setup to avoid twisting of the cables. A computer program implemented in C language was used to control the orbital radius and orbital rate of the mother satellite, and the inclination angle of the table. A piece of dry ice was placed under the subsatellite model to reduce friction between the subsatellite and the table. As the result of the dry ice, the damping ratio was reduced to approximately 1.97×10^{-2} for the case of an inclination angle of 15 deg, which is small enough to emulate the librational motion of the tethered system. A camera is installed above the table to record data to produce a bifurcation diagram for the tether angle. To easily obtain photographs of the subsatellite, the walls of the apparatus were covered by dark curtains. A counter weight was installed on the opposite side of the table to maintain the balance during rotation.

IV. Results of Numerical Simulations and Experiments

A. Numerical Results

Numerical simulations for the pitch motion were carried out using the parameters listed in Table 2. In this Note, the fourth-order

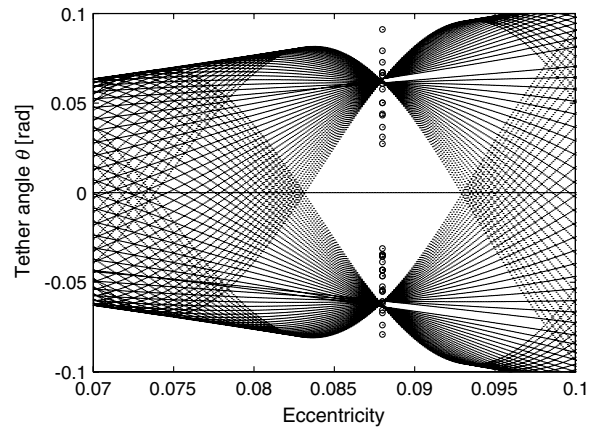


Fig. 8 Tether angles at the perigee for 50 orbits determined from experiments for $e = 0.088$ (shown as circles), along with numerical results for $e = 0.07$ to 0.1.

adaptive step-size-controlled Runge–Kutta scheme (ode 45) provided by MATLAB was used in order to calculate the pitch motion. Figure 7 shows a bifurcation diagram for the eccentricity range 0.0 to 0.45 for the case of 100 orbits. Some periodic motions are observed, which may correspond to the ones listed in Table 1. The eccentricity value of 0.345 for periodic motion with a period of three orbits is similar to the value of 0.24966 derived from Eq. (1) for a period of three orbits. It can also be seen that the divergence which occurs at an eccentricity of 0.39 is quite similar to that in Fig. 2 for a eccentricity of 0.314, and that the pitch motion changes from librational to rotational when the eccentricity is greater than about 0.39. This boundary value of eccentricity is greater than the value of 0.314 derived from Eq. (1). This may be because the effect of the emulated orbital eccentricity in the simulation is smaller than that based on Eq. (1) in the numerical simulation. Some periodic motions were selected from the bifurcation diagram (Fig. 7), and the corresponding eccentricities are listed in Table 3.

B. Experimental Results

As mentioned earlier, the tether is assumed to be rigid. However, since the tether used in the experiments is a string, it is possible for it to become slack for the case of high eccentricity, because the orbital radius of the mother satellite changes very quickly in such a situation, whereas it is impossible to completely eliminate the friction between the dry ice under the subsatellite and the inclined turntable. By taking this into consideration, and by referring to the numerical results, we chose an eccentricity of $e = 0.088$, which is small enough to easily emulate librational motion in the experimental setup and a quite clear periodic motion with a period of two orbits is observed in the bifurcation resulting from the equation of motion based on the apparatus. If the emulated semimajor axis corresponds to 8000 km, then the orbital period is 7121 s. In this case, the orbital motion is reproduced in the experiments by a factor of 1360.

Table 3 Eccentricities for periodic motions

| Period (orbits) | Eccentricity |
|-----------------|--------------|
| 2 | 0.088 |
| 4 | 0.215 |
| 3 | 0.345 |

The tether angles at the perigee resulting from the experiments over 50 orbits are indicated by the symbol \circ in Fig. 8, which, for comparison, also shows the numerical results for eccentricities in the range 0.07 to 0.1. The quasi-periodic motions with a period of two orbits, which was predicted from the numerical simulations based on the experimental parameters, are successfully observed in the experiment.

V. Conclusions

A ground-based apparatus was proposed and developed to study in-plane periodic motions of a tethered satellite system in elliptic orbits. The equation of motion for the apparatus was derived and the inclination angle of the turntable was determined in accordance with the orbital elements to emulate the gravity gradient affecting the tethered satellite system.

Numerical simulations were then carried out to test the validity of the derived equation of motion. The results of numerical simulations showed that the derived equation of motion based on the experimental setup is capable of emulating the periodic motion of a tethered satellite system in elliptic orbits, but slight differences exist between the eccentricities corresponding to the periodic motion. This may be because the emulated gravity gradient on the subsatellite is larger than that of the corresponding orbit. One experimental case study was carried out, and the experimental results showed that the experimental setup can emulate librational pitch motion of a tethered satellite system for the case of small eccentricity. However, emulation of librational motion for high eccentricity cases still remains an open problem.

Further studies are under consideration using the presented experimental setup, with intention to investigate applications of delayed feedback control using a variable tether length and electric current on tether to chaotic pitch motion control of electrodynamic tether systems in elliptic orbits. In addition, it would be of interest to perform simulations of debris capture and subsatellite release missions.

Acknowledgments

This study was supported in part by a grant from the Kurata Memorial Hitachi Science and Technology Foundation, and in part by Grants for Researchers Attending International Conferences from NEC C&C Foundation.

References

- [1] Sorensen, K., "Conceptual Design and Analysis of an MXER Tether Boost Station," AIAA/SME/SAE/ASEE Joint Propulsion Conference, AIAA Paper 2001-3915, 2001.
- [2] Forward, R. L., Hoyt, R. P., and Upoff, C. W., "Terminator Tether: A Spacecraft Deorbit Device," *Journal of Spacecraft and Rockets*, Vol. 37, No. 2, 2000, pp. 187–196.
- [3] Cosmo, M. L., and Lorenzini, E. C., "Tether In Space Handbook, Third Edition," *Smithsonian Astrophysical Observatory*, NASA Marshall Space Flight Center, Huntsville, AL, 1997.
- [4] Higuchi, K., and Natori, C. M., "Ground Experiment of Motion Control of Retrieving Space Tether," AIAA/ASME/ASCE/AHS/ASC Structures, Structural Dynamics, and Materials Conference, AIAA Paper 1997-1217, 1997.
- [5] Koga, N., "Analysis on Deployment Control of Tethered Subsatellite System in the Effect of Rotational Field," *Advances in the Astronautical Sciences*, Vol. 96, 1997, pp. 103–109.
- [6] Swan, P. A., "Dynamics and Control of Tethers in Elliptical Orbits," Ph.D., Dissertation, Univ. of California, Los Angeles, CA, 1984.
- [7] Karasopoulos, H., and Richardson, D. L., "Chaos in the Pitch Equation of Motion for a Gravity-Gradient Satellite," AIAA/AAS Astrodynamics Conference, AIAA Paper 92-4369, 1992.
- [8] Peláez, J., and Lara, M., "Periodic Solutions in Rigid Electrodynamic Tethers on Inclined Orbits," *Journal of Guidance, Control, and Dynamics*, Vol. 26, No. 3, 2003, pp. 395–406.
doi:10.2514/2.5077
- [9] Peláez, J., and Andres, Y. N., "Dynamics Stability of Electrodynamic Tethers in Inclined Elliptical Orbits," *Journal of Guidance, Control, and Dynamics*, Vol. 28, No. 4, 2005, pp. 611–622.
doi:10.2514/1.6685
- [10] Pyragas, K., "Continuous Control of Chaos by Self-Controlling Feedback," *Physics Letters A*, Vol. 170, No. 6, 1992, pp. 421–428.
doi:10.1016/0375-9601(92)90745-8
- [11] Peláez, J., and Lorenzini, E. C., "Libration Control of Electrodynamic Tethers in Inclined Orbit," *Journal of Guidance, Control, and Dynamics*, Vol. 28, No. 2, 2005, pp. 269–279.
doi:10.2514/1.6473
- [12] Kojima, H., Iwasaki, M., Fujii, H. A., Blanksby, C., and Trivailo, P., "Nonlinear Control of Librational Motion of Tethered Satellites in Elliptic Orbits," *Journal of Guidance, Control, and Dynamics*, Vol. 27, No. 2, 2004, pp. 229–239.
doi:10.2514/1.9166
- [13] Iñarrea, M., and Peláez, J., "Libration Control of Electrodynamic Tethers Using the Extended Time-Delayed Autosynchronization Method," *Journal of Guidance, Control, and Dynamics*, Vol. 33, No. 3, 2010, pp. 923–933.
doi:10.2514/1.44232
- [14] Kojima, H., and Sugimoto, T., "Stability Analysis of In-Plane and Out-of-Plane Periodic Motions of Electrodynamic Tether System in Inclined Elliptic Orbit," *Acta Astronautica*, Vol. 65, Nos. 3–4, 2009, pp. 477–488.
doi:10.1016/j.actaastro.2009.02.006
- [15] Kojima, H., and Sugimoto, T., "Switching Delayed Feedback Control for an Electrodynamic Tether System in an Inclined Elliptic Orbit," *Acta Astronautica*, Vol. 66, Nos. 7–8, 2010, pp. 1072–1080.
doi:10.1016/j.actaastro.2009.09.014
- [16] Hughes, P. C., *Spacecraft Attitude Dynamics*, Wiley, New York, 1986, pp. 308–313.
- [17] Kojima, H., "Conceptual Design of Ground Based Electrodynamic Tether Simulator," *Proceedings of the 37th JSASS Annual Meeting*, Tokyo, 2006, pp. 245–248 (in Japanese).